OMAE2020-18759

TIME DOMAIN VIV ANALYSIS TOOL VIVANA-TD: VALIDATIONS AND IMPROVEMENTS

Jie Wu[1], Jingzhe Jin, Decao Yin, Halvor Lie, Elizabeth Passano
SINTEF Ocean
Trondheim, Norway

Svein Sævik
NTNU
Trondheim, Norway

Michael A Tognarelli
BP America Production
Houston, USA

Guttorm Grytøyr
Equinor
Oslo, Norway

Torgrim Andersen
Kongsberg Maritime
Asker, Norway

Daniel Karunakaran
Subsea7
Stavanger, Norway

Ragnar Igland
Aker Solutions,
Trondheim, Norway

ABSTRACT

An empirical time-domain (TD) vortex-induced vibration (VIV) prediction model has been implemented in a software called VIVANA-TD based on its earlier development by Thorsen at NTNU. It models the synchronization of VIV loads and structural responses with a set of empirical parameters generalized from model tests. Combining this time domain hydrodynamic load model with a non-linear finite element structural model makes it possible to account for structural non-linearities and time-varying flow.

A joint industry project (JIP), i.e., Lazy Wave Riser JIP has been organized to improve the design basis for SLWRs. This JIP is executed by SINTEF Ocean with support from NTNU. The industry participants are Equinor, BP, Subsea7, Kongsberg Maritime and Aker Solutions. The overall objective of this JIP is to systematically validate VIVANA-TD, in order to establish it as an industrial tool for VIV prediction. It is also aimed to improve the empirical basis and methods for calculation of VIV of deep-water steel lazy wave risers (SLWRs).

In the present paper, the validation study is presented for selected model tests in constant flow conditions with uniform and sheared profiles. The test model includes bare pipe, pipe with partial strake coverage and riser model with staggered buoyancy elements. The empirical parameters have been generalized based on extensive model test data. Limitations and improvement of the model have been also been explored. The results show that the present TD model can represent reasonably the VIV loads and that the prediction has good agreement with measurements in general.

Keywords: VIV, Time Domain Prediction, Steel Lazy Wave Risers, VIVANA-TD

NOMENCLATURE

$\bar{f}$	Non-dimensional frequency
$\bar{f}_0$	Non-dimensional frequency center of the synchronization range in TD VIV model
$\bar{f}_{min}$	Lower limit of the synchronization range
$\bar{f}_{max}$	Higher limit of the synchronization range
f_n	Natural frequency
f_{osc}	Oscillation frequency
$\Delta\bar{f}$	Non-dimensional frequency of the synchronization range defined by $\bar{f}_{min}$ and $\bar{f}_{max}$
$\emptyset_{\dot{y}_{rel}}$	Instantaneous phase of the relative cross-flow velocity of the structure in TD VIV model
$\emptyset_{v,y}$	Instantaneous phase of the cross-flow vortex-shedding force in TD VIV model
θ	Instantaneous phase difference between the structure's relative cross-flow velocity and the cross-flow vortex-shedding force
ρ	Density of fluid
D	Outer diameter of the cylinder
D_b	Diameter of the buoyancy element
D_r	Diameter of the bare riser section
L	Length of the cylinder
L_b	Length of the buoyancy element
L_r	Length of the bare riser section
U	Flow speed

---

[1] Contact author: jie.wu@sintef.no

U_{rn}	Reduced velocity
A	Displacement amplitude
A/D	Amplitude to diameter ratio
C_A^n	Added mass coefficient normal to the flow direction
C_A	Added mass coefficient
C_D	Cross-flow drag coefficient
C_D^n	Drag coefficient normal to the flow direction
C_e	Excitation coefficient
$C_{v,y}$	Cross-flow vortex shedding force coefficient
$F_{v,y}$	Cross-flow vortex shedding force
$F_{damp,y}$	Cross-flow damping force
$F_{inertia,y}$	Cross-flow inertia force
F_x	Drag force
F_y	Lift force
P	Pitch of the strake
H	Height of the strake
$\mathbf{r}$	Nodal displacement vector in the dynamic equilibrium equation
$\dot{\mathbf{r}}$	Nodal velocity vector in the dynamic equilibrium equation
$\ddot{\mathbf{r}}$	Nodal acceleration vector in the dynamic equilibrium equation
$\mathbf{C}$	Damping matrix in the dynamic equilibrium equation
$\mathbf{K}$	Stiffness matrix in the dynamic equilibrium equation
$\mathbf{M}$	Mass matrix in the dynamic equilibrium equation
$\mathbf{Q}$	External force vector in the dynamic equilibrium equation
CF	Cross-flow
IL	In-line
JIP	Joint industry project
NTNU	Norwegian University of Science and Technology
SCR	Steel catenary riser
SLWR	Steel lazy wave riser
FD	Frequency domain
TD	Time domain
TDP	Touch-down point
VIV	Vortex-induced vibration

1 INTRODUCTION

A steel catenary riser (SCR) is a catenary shaped connection between a subsea pipeline and a floating or fixed production platform. A SLWR is a special SCR configuration. A typical SLWR consists of four segments, namely the hang-off and sag-bend segment, the buoyancy segment and the touchdown segment. The buoyancy segment is equipped with external buoyancy elements, which provides buoyancy forces in excess of the weight. To reduce VIV, suppression devices such as strakes are often used. Sketch of a typical SLWR is shown in Figure 1-1.

SLWRs can be a possible solution for recent deep-water production systems. This type of risers can be less costly than flexible risers and offers sufficient flexibility to allow for floater motions. Their advantage relative to ordinary SCR is not only the

increased flexibility, but also that the dynamic response at the touch down point (TDP) is significantly reduced with a decrease of fatigue accumulation at this hot spot as consequence.
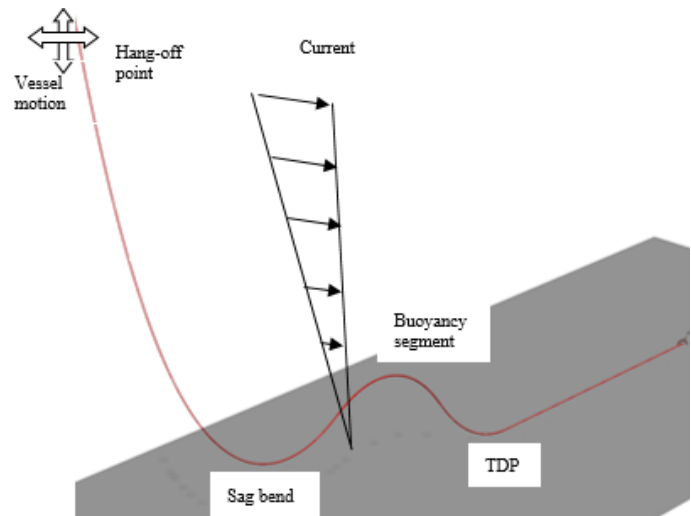

Figure 1-1 Example configuration of SLWR.

Design verification of a production riser on a floating production unit must include calculation of fatigue damage during its lifetime. Three sets of analyses might be carried out:

- Dynamic response from wave forces along the riser combined with motions of the hang-off point. This type of analysis might apply an integrated calculation of riser dynamics and floater motions
- VIV from stationary current without any influence from waves and floater motions
- VIV caused by motions at the hang-off point without any influence from current

A new empirical method for TD calculation of VIV has been developed by Thorsen [1]. The empirical parameters in this method are closely related to the physics observed from VIV model tests. A synchronization model introduces a phase-coupling between the force and response, which effectively captures how the local vortex shedding frequency may increase or decrease to obtain lock-in. Combining this hydrodynamic load model with a non-linear finite element structural model makes it possible to account for time-varying flow and structural non-linearities, e.g., seabed contact. This approach provides improved prediction compared to the use of a set of frequency domain (FD) analyses to account for variation of the flow velocity. A review of the recent research related to VIV of SLWRs can be found in [2].

2 OBJECTIVE

The key objectives of Lazy Wave Riser JIP are the following:

1) Qualify the VIVANA-TD software for VIV prediction subjected to both constant current and vessel motions, that can be used in design by industry

2) Define an empirical basis and rational methods for calculation of VIV for SLWRs

3) Define a road map towards future integrated model for combined waves and VIV loads

During the development of the TD load code at NTNU, different modelling choices have been studied in order to provide a robust model which relies on as few as possible empirical parameters. This also led to changes in the use of empirical parameters. The latest code has been implemented in VIVANA-TD.

Therefore, the main objective of this paper is to present the validation study of VIV in constant flow conditions.

3   VALIDATION METHODOLOGY

3.1   Principle

In accordance with the basic principles adopted in the most recognized rules this study targets unbiased estimates of VIV. This means that empirical data and models are based on the best fit principle. Any uncertainty and modelling error are to be accounted for in the safety factors.

Standard design safety factors e.g. design fatigue factor, will have to be established by further work. The cross-flow (CF) response is the focus at the present stage. In-line (IL) response is not evaluated due to the relatively larger uncertainty in the combined CF and IL load model.

The validation is carried out in an iterative process:
- Examine the TD load formulation.
- Derive empirical parameters from rigid cylinder tests.
- Validate VIVANA-TD against selected elastic pipe tests.

In some cases, the empirical parameters are adjusted based on results from elastic pipe test.

3.2   Evaluation parameters

In the validation, the predicted frequency content, displacement standard deviation, curvature standard deviation and fatigue damage are compared with measurements.

In the processing of the model test data, a time window has been selected where the towing speed reaches the target value and the initial/end transient phase have been excluded. The displacement is estimated by double integration of the measured acceleration signal. The curvature is derived from the bending strain measurement.

Filtering has been applied to both the simulation results and measurements with focus on the CF responses at the primary shedding frequency.

The dominating frequencies were taken as the peak frequencies in the curvature spectra at the positions along the riser with maximum CF curvature standard deviation.

The stress was derived from the curvature and the fatigue damage was calculated from the stress time histories using the rain-flow counting method. The maximum measured fatigue damage was taken from the highest fatigue damage of all the measured signals. The maximum predicted fatigue damage was taken from the highest fatigue damage of the numerical model corresponding to the same measurement locations.

4   THEORY OF THE TIME DOMAIN MODEL

The TD VIV prediction model has been developed by Thorsen [1], who focused on the CF VIV load model. Ulveseter, et al [3] extended the load model to describe the combined CF and IL response, as well as the pure IL responses relevant for the free spanning pipelines. The higher harmonic loads have also been modelled. In the present work, the CF load model will be evaluated. The results will provide inputs to validate the combined CF and IL load model in the future. The theoretical background of the CF time domain VIV model is summarized in this section.

For a cylinder subjected to an incoming flow, vortices will be shed from both sides of the cylinder, which leads to periodic forces in IL and CF directions, as shown in Figure 4-1. $\dot{x}$ and $\dot{y}$ are the CF and IL velocities of the cross-section and $\ddot{x}$ and $\ddot{y}$ are the CF and IL accelerations of the cross-section.
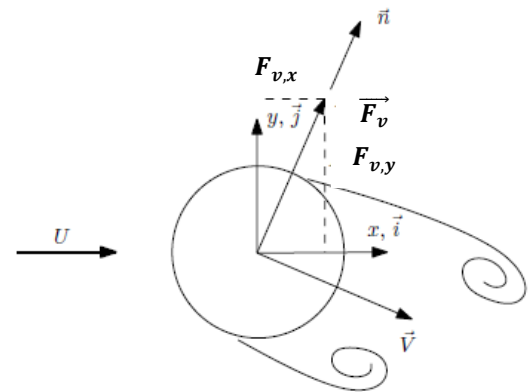

Figure 4-1 Definition of the coordinate system for the TD VIV model

4.1   Vortex shedding force and synchronization model

Considering the vortex shedding force in the CF first, the force model can be described by:

$$F_{v,y} = \frac{1}{2}\rho D C_{v,y}|v_n|(j_3 \times v_n)cos\emptyset_{v,y} \qquad \textbf{Equation 4-1}$$

Where D is the diameter of the cylinder, $\emptyset_{v,y}$ is the instantaneous phase of the CF vortex shedding force and v_n is the relative velocity normal to the cylinder. The force $F_{v,y}$ points in the direction normal to the relative flow velocity. The magnitude of the force is determined by a dimensionless coefficient, $C_{v,y}$, and the oscillatory behavior is taken into account through the time varying instantaneous phase $\emptyset_{v,y}$.

As the vortex shedding force oscillates, the phase $\emptyset_{v,y}$ changes continuously, and goes from 0 to 2π in one complete

cycle. If the frequency of the force was some constant f_v, the rate of change of the phase angle would be $\emptyset_{v,y} = 2\pi f_v$. This is however not the case, as the frequency is influenced by, and will in some cases synchronize with the cylinder motion.

A synchronization model introduces a phase-coupling between the force and response, which effectively captures how the local vortex shedding frequency may increase or decrease to obtain lock-in.

The instantaneous frequency of the CF vortex shedding force is given by:

$$\frac{d\emptyset_{v,y}}{dt} = 2\pi f_{v,y} = \frac{2\pi|v_n|}{D}\bar{f} \qquad \text{Equation 4-2}$$

where

$$\bar{f} = \bar{f}_0 + \Delta\bar{f}\sin(\theta) \qquad \text{Equation 4-3}$$

$$\theta = \emptyset_{\dot{y}_{rel}} - \emptyset_{v,y} \qquad \text{Equation 4-4}$$

$\bar{f}_0$ and $\Delta\bar{f}$ determines the position and span of the synchronization range, respectively. $\emptyset_{\dot{y}_{rel}}$ is the instantaneous phase of the (local) CF structural velocity. θ describes the difference between the instantaneous phase of the vortex shedding force and the phase of the structural velocity in the local CF direction.

4.2 Damping model

The hydrodynamic damping force model is dependent on the relative speed in the direction normal to the cylinder and a drag coefficient, as described by Equation 4-5. The net energy of the system will be determined by the combination of the vortex shedding force term and the damping force term.

$$F_{damp} = \frac{1}{2}\rho C_D D v_n|v_n| \qquad \text{Equation 4-5}$$

4.3 Added mass model

In a constant flow, the inertial force is defined by

$$F_{inertia} = -C_A\rho\frac{\pi D^2}{4}\ddot{x}_n \qquad \text{Equation 4-6}$$

As discussed earlier, part of the vortex shedding force will in addition also contribute to the inertial force.

4.4 Complete load formulation

The total hydrodynamic load model consists of the force term due to water particle acceleration, an added mass term, a damping force term and a vortex shedding force term. Note that the force model includes both IL drag force, inertia force and CF VIV force. It can be considered as the normal Morison equation formulation with a vortex shedding force term in addition.

The CF VIV force (F) model is presented below:

$$F = (C_A + 1)\rho\frac{\pi D^2}{4}\dot{u}_n - C_A\rho\frac{\pi D^2}{4}\ddot{x}_n + \frac{1}{2}\rho C_D D v_n|v_n| +$$
$$\frac{1}{2}\rho D C_{v,y}|v_n|(j \times v_n)\cos\emptyset_{v,y} \qquad \text{Equation 4-7}$$

4.5 Solving dynamic equilibrium equation

The system dynamic equilibrium equation is solved in time domain.

$$M\ddot{r} + C\dot{r} + Kr = Q \qquad \text{Equation 4-8}$$

where, M, C and K are the mass, damping and stiffness matrix respectively; and r, $\dot{r}$ and $\ddot{r}$ are the displacement, velocity and acceleration vectors respectively; Q is the load vector.

The response is solved in a step-by-step numerical integration of the incremental dynamic equilibrium equations, with a Newton-Raphson type of equilibrium iteration at each time step. This approach allows for a proper treatment of all the described nonlinearities.

5 DERIVATION OF EMPIRICAL HYDRODYNAMIC PARAMETERS BASED ON RIGID CYLINDER TEST DATA

There have been extensive experimental studies on VIV responses of both rigid cylinders and elastic pipes subjected to a constant flow. The rigid cylinder tests are often carried out with free oscillation setup on elastic supports or forced motions [34], [35]. The motion direction is often restricted in one direction (1D). 2D tests [29], [30], [37] show that CF response is strongly influenced by the response in the IL direction. Prediction based on the combined IL and CF load model is still under research [16], [40]. Prototype Reynolds number can be achieved in some of the 1D tests [42] - [44], which show that VIV responses are affected by Reynolds number and surface roughness, especially in the critical Reynolds number regime. No complete hydrodynamic database at prototype Reynolds number exists considering the large parameter space.

The elastic pipe VIV tests provide better understanding of the global responses compared to a rigid cylinder section, e.g. [21], [22], [45]. The hydrodynamic coefficients are associated with trajectories of the motions along the elastic pipe [8], [9], [26]. When vibrating at high modes, the response becomes increasingly non-stationary. The response frequency may vary both in time (time-sharing) and along the length of the structure (space sharing)[23], [24]. The responses are further influenced by the bending stiffness, mode order and the presence of the travelling waves, etc. [20] Efforts to derive hydrodynamic coefficients directly from elastic pipe responses have been made [18], [27]. Most of the elastic pipe VIV tests are carried out at sub-critical Reynolds numbers. Field measurements normally have larger uncertainties due to more complex environmental load and structure response patterns and relatively lower measurement resolution as compared to the tests in the laboratories [19].

When a SLWR is subjected to current, both the buoyancy elements and the riser may experience VIV. The vortex shedding process from the riser and the buoyancy element will also interact. The illustration of the buoyancy segment of the SLWR is shown in Figure 5-1.
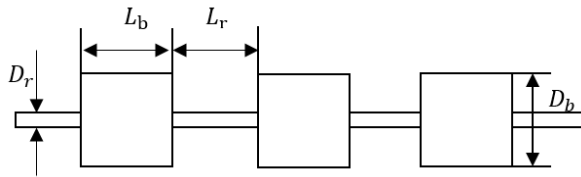
Figure 5-1 Illustration of the staggered buoyancy elements.

Several model tests were carried out to study the interaction of bare pipe section and buoyancy elements and its effect on VIV [31], [32], [33], [38]. The study of the test data shows that the interaction can be influenced by several geometry parameters, e.g., L_b/D_b, L_r/D_r, L_r/L_b, etc. There is a competition between the vortex induced forces acting on the buoyancy element and the riser segment. A rigid cylinder forced motion experiment [39] was carried out in order to obtain hydrodynamic data for riser with staggered buoyancy elements in constant flow for two configurations.

The derivation of the empirical parameters is based on consolidation of publicly available rigid cylinder test data. Several rigid cylinder model tests have been used to derive empirical parameters in the time domain prediction model. The empirical parameters were firstly derived from the forced motion test data of a rigid cylinder subjected to pure CF motions and thereafter used to predict response of rigid cylinder subjected to pure CF and combined IL&CF motions, respectively. The parameters were then applied to predict VIV responses of elastic pipes in the validation study in the Section 6.

5.1 Empirical parameters for bare cylinder

Based on the discussion above, it is difficult to generalize the empirical parameters based on one single model test. These parameters were therefore derived by combined application of data from both forced motion tests and free oscillation tests with elastic supports.

5.1.1 Derivation of parameters based on forced motion test with pure CF motions

The hydrodynamic parameters required by the prediction tools are normally generalized from rigid cylinder forced motion tests. In such tests, a rigid cylinder is towed through the water at a constant speed (U) and forced to oscillate under designed motion amplitudes (A) and frequencies (f_{osc}), which are approximating the actual trajectories of the cross-section of a flexible pipe. The measured hydrodynamic force of the rigid cylinder section is normally decomposed into inertia (in-phase with acceleration) and excitation force (in-phase with velocity) components. The normalized excitation coefficient (C_e) and the added mass coefficient (C_a) are then derived[17]. Despite the efforts to obtain hydrodynamic data from realistic cylinder motions [16], [29], [40], the hydrodynamic parameters used in the present prediction tools are still based on tests with one-dimensional CF harmonic motions.

A well-known forced motion test with pure CF motions was carried out by Gopalkrishnan [17]. Different TD empirical parameter values have been evaluated by Thorsen [1] so that the corresponding excitation and added mass coefficients can represent the hydrodynamic coefficient data from this model test. However, the synchronization function in the TD model has been simplified during the development. The selected TD parameter values are presented in Table 5-1. The excitation coefficient is related to both the vortex shedding force term ($F_{v,y}$) and the damping force term (F_{damp}), as explained in the Section 4. The added mass coefficient is associated with the other part of the vortex shedding force term ($F_{v,y}$) and the inertia force term ($F_{inertia}$). The phase between the vortex shedding force ($F_{v,y}$) and relative flow velocity was determined by the synchronization function for a given excitation range in terms of the non-dimensional frequency ($\bar{f}_{min} - \bar{f}_{max}$).

The comparison between the excitation coefficient contour from the forced motion test and the reproduced data based on empirical TD parameters are presented in Figure 5-2. As shown in Figure 5-2 a), the maximum positive excitation coefficient (C_e=0.78) occurs at amplitude ratio A/D about 0.5 and non-dimensional frequency about $\bar{f}$=0.17. The C_e=0 contour is marked by the thick line in the figure. The corresponding highest A/D value is about 0.84 around $\bar{f}$=0.175. Positive excitation coefficient values are observed within $0.125 < \bar{f} < 0.3$. The excitation coefficients based on the TD parameters are presented in Figure 5-2 b).

Table 5-1 TD parameters for a bare cylinder based on forced motion test data

Structure type	Parameters					
	$C_{v,y}$	C_D	C_A	$\bar{f}_0$	$\bar{f}_{min}$	$\bar{f}_{max}$
Bare	1.2	1.1	1.0	0.18	0.11	0.26

The cylinder with no material damping subjected to VIV will reach steady state responses when the net energy transfer between fluid and structure is zero. The corresponding steady state response amplitude ratio can be indicated by the zero-excitation contour line. The comparison shows that the TD parameters will lead to about the same max A/D at $\bar{f}$=0.175 and higher A/D in general, as shown in Figure 5-2.
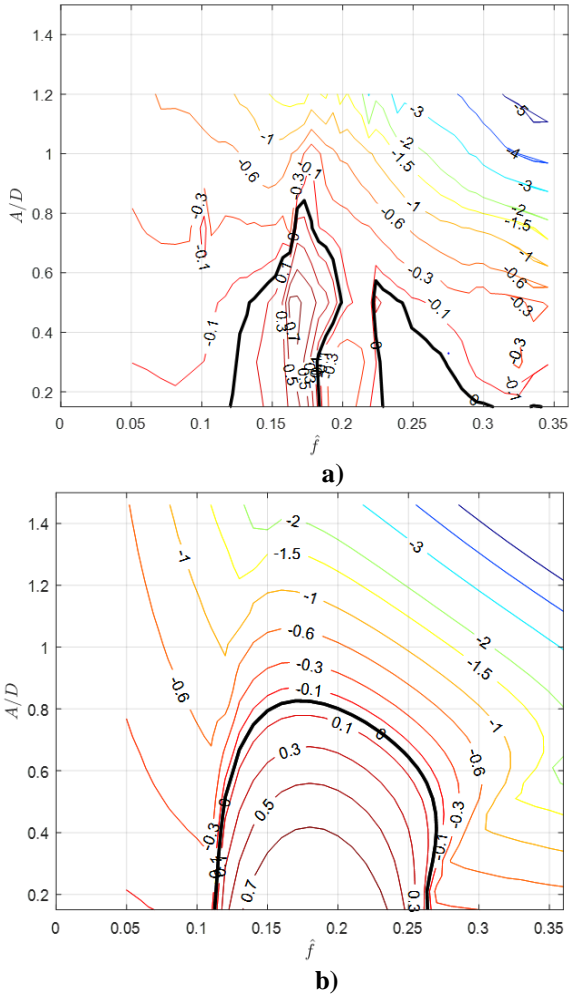
Figure 5-2 Excitation coefficient contour plots. a) Forced motion test data; b) Coefficients based on the time domain model

The added mass coefficient data comparison is presented in Figure 5-3. High added mass values ($C_A > 3$) are observed at low A/D values.

It is not intended to achieve perfect agreement between the test data and the results based on the TD model. This results from the modelling choice made for the CF load formulation which is determined by 6 parameters and the synchronization function, which aims to reflect the characteristics of VIV load and synchronization by a minimum number of empirical parameters.

In order to test and explore the TD model, the parameters defined based on the forced motion test data were used to predict CF response of a rigid cylinder with elastic support. The simulation results were compared to model test results from an elastic rigid cylinder VIV test.
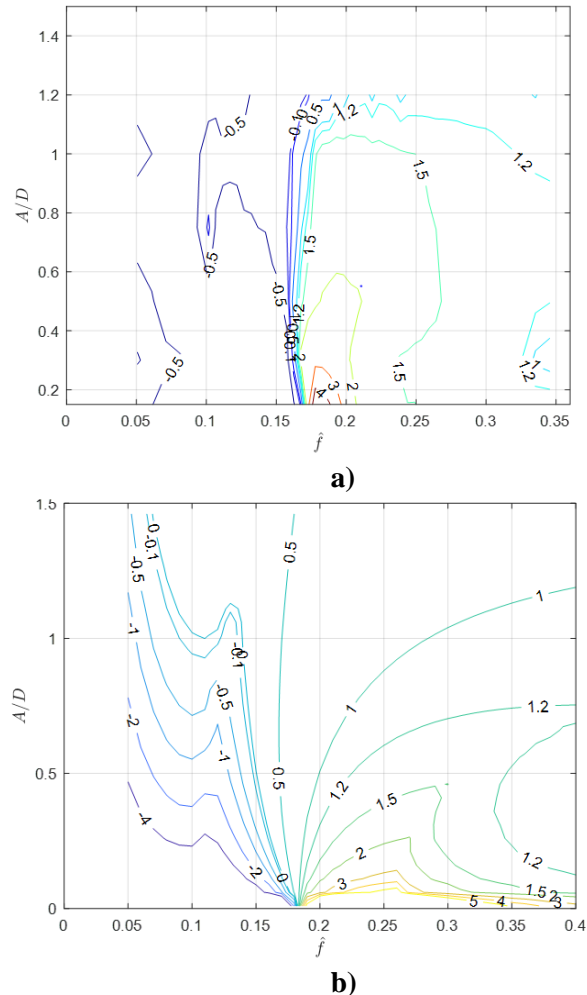
Figure 5-3 Added mass coefficient contour plots. a) Forced motion test data; b) Coefficients based on the time domain model

Vikestad's test set-up [34] was modelled with the key parameters listed in the Table 5-2. The measured displacement amplitude ratio (A/D) and added mass (C_A) values were extracted from the thesis work where the highest A/D was found to be 1.13. Free oscillation tests with similar test parameters ([30], [35], [36]) also show maximum A/D in the range of 0.9 – 1.2.

The predicted amplitude ratio (A/D) has been reported in Figure 5-5. The red data points in the figure represent response predicted by using the parameters based on the forced motion test data, refer to Table 5-1. It can be seen that the highest predicted A/D is 0.84 and the corresponding $\bar{f}$ is 0.17, which is consistent with the forced motion test results shown in the Figure 5-4.

Table 5-2 Vikestad's model test parameters

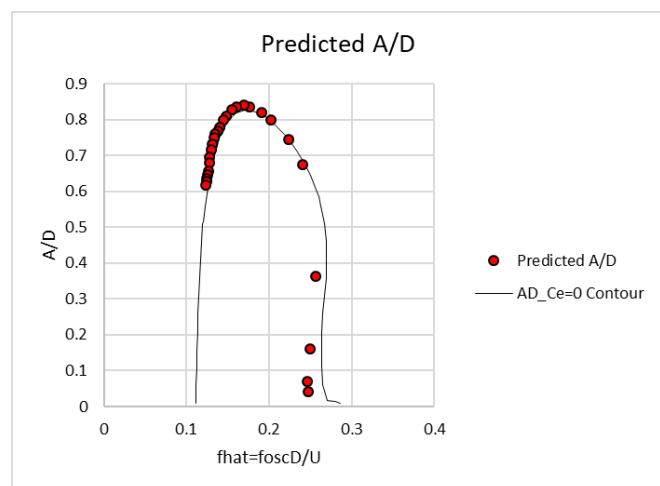| Parameters	Value	Unit
Diameter	0.1	m
Length	2	m
Total stiffness	415	N/m
Effective dry mass	13.06	kg/m
Natural frequency in still water	0.498	Hz
Mass ratio	1.7	
Damping ratio in water with cylinder	0.014	

Figure 5-4 Comparison of predicted A/D and zero excitation coefficient contour line

But, the predicted maximum A/D is smaller than the free oscillation test data ($A_{max}/D = 1.15$), as represented as the squared data points in Figure 5-5. The difference may be related to the setup between forced and free oscillation test. The motion of an elastic mounted cylinder may not be entirely harmonic compared to the forced motion test, which can lead to difference in the hydrodynamic forces and motion amplitude, among other factors. It is also noted that the response in the high reduced velocity region ($U_{rn} = U/f_n D > 8.7$) is over-predicted.

Differences can also be seen in the added mass between the estimated values from prediction and the test data, as shown in Figure 5-6. The empirical parameters based on the forced motion test data (red data points) lead to significantly lower added mass values for $U_{rn} < 5$ and slightly higher values for higher U_{rn}. This is considered of less importance for the riser VIV responses, but more relevant for prediction of the free spanning pipeline at low U_{rn}.
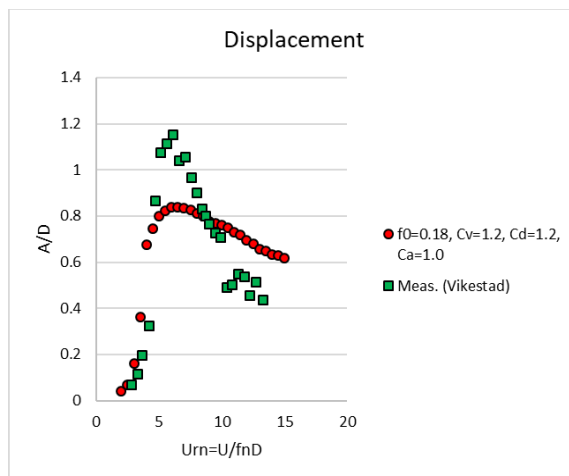
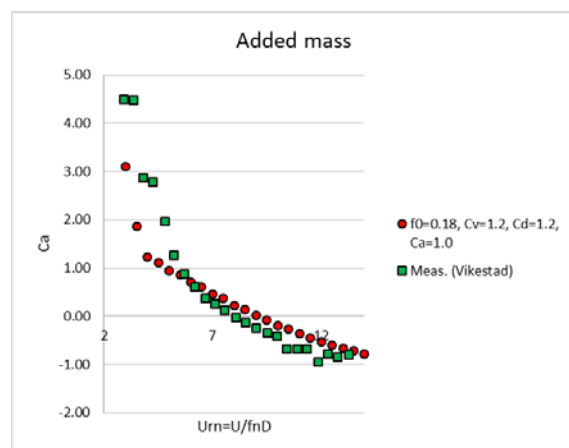**Figure 5-5 Comparison of A/D prediction against model test data from Vikestad**

Figure 5-6 Comparison of added mass prediction against model test data from Vikestad

5.1.2 Modification of empirical parameters for the bare cylinder

When the cylinder is allowed to oscillate in both CF and IL directions, the corresponding VIV response and hydrodynamic coefficients will be different compared to tests with 1D motions. One of the key changes is that the peak excitation occurs at a lower $\bar{f}_0$. Dahl [30], Sarpkaya [37], Søreide [37] reported $\bar{f}_0$ in the range of 0.1 – 0.14, when there is combined CF and IL motions in their tests.

Therefore, the empirical parameters are modified to account for difference in the test setup between forced motion and free oscillation test and the additional effects due to the 2D motions. The parameter $C_{v,y}$, C_D, $\bar{f}_0$ and $\bar{f}_{min}$ values have been adjusted accordingly. The corresponding excitation coefficients are presented in Figure 5-7.
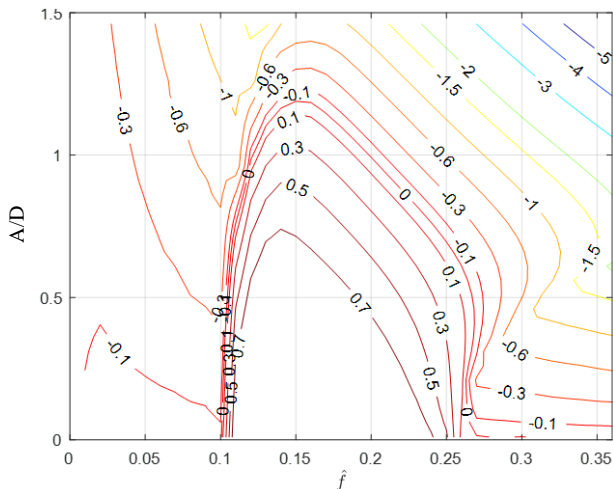
Figure 5-7 Excitation coefficient based on adjusted empirical TD parameters

The prediction with modified empirical parameters is presented as the blue data points in Figure 5-8. The $C_{v,y}$ value has been increased and C_D value reduced, which means higher excitation force and lower damping force. The predicted A/D increases from 0.84 to 1.2 or 43% higher than the original prediction.

This set of parameters are further used in the validation study of elastic pipes for bare pipe sections. Note that different parameters are used for the bare pipe sections between staggered buoyancy elements. This is due to additional hydrodynamic effects, which are further discussed in the Section 5.2.
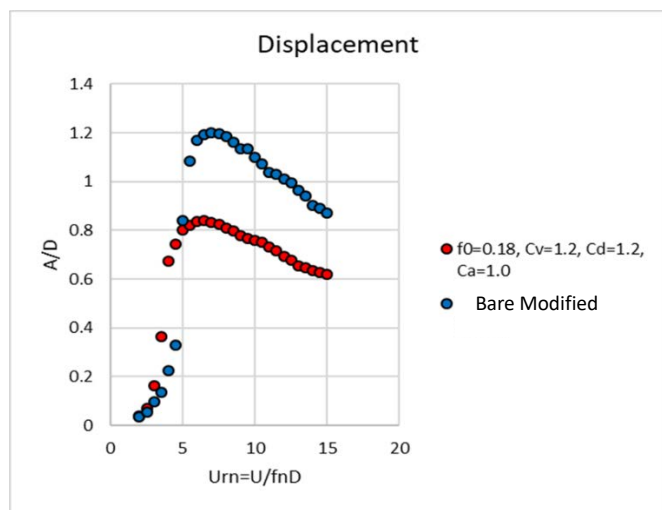
Figure 5-8 Prediction based on adjusted empirical parameters

5.2   Empirical parameters for staggered buoyancy elements

The empirical parameters have been derived based on the measured pure CF hydrodynamic force coefficients for two of

the staggered buoyancy element configurations [39]. The length of the bare riser section (L_r) is the same or twice of the length of the buoyancy element (L_b) in these two configurations, as shown in Figure 5-1. The diameter of the buoyancy element (D_b) is five times that of the bare riser (D_r).

The TD parameters are determined based on the characteristic values in the experimental data, i.e., 1) excitation region in terms of non-dimensional frequency, 2) the value of the peak excitation coefficient and its corresponding non-dimensional frequency, 3) the maximum amplitude ratio corresponding to the zero excitation coefficient.

Similar TD parameters were derived for the buoyancy element configuration ($L_b/L_r=1/2$). The hydrodynamic parameters of the bare riser section are similar to those of a bare pipe without buoyancy elements as expected.
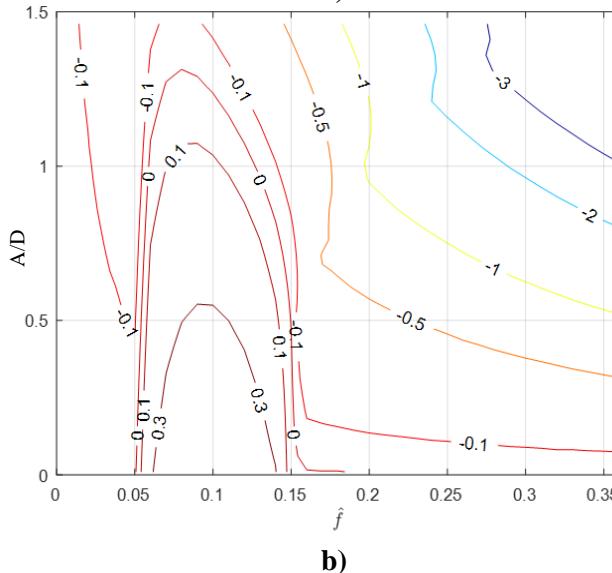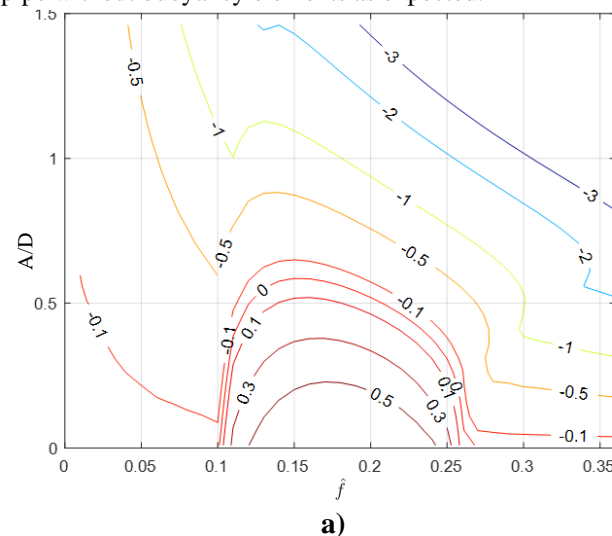

a)

b)

Figure 5-9 Generated excitation coefficient contour plots based on forced motion test data for Config. ($L_b/L_r = 1/1$). a): Bare riser section; b): Buoyancy element

5.2.1 Empirical parameters for strakes

Drengsrud [10] studied the modelling of strakes in VIVANA-TD. The hydrodynamic coefficients were estimated from analytical formulations proposed by Nestegård et al. [11], which shows reasonable agreement with experimental results [47]. For a riser partially covered with strakes, the riser model is divided into bare and straked segments, where the TD VIV and Morison load model are applied respectively. Hydrodynamic drag and added mass coefficients are required as input to both the TD VIV load model and the Morison load model, and how they are established is presented below.

Table 5-3 Hydrodynamic coefficients for strake
($P/D = 17.5, H/D = 0.25$)

Parameters	Values
Drag coefficient normal to the flow direction C_D^n	1.935
Added mass coefficient normal to the flow direction C_A^n	1.508

6 VALIDATION RESULTS

Two model tests are selected based on the data quality, relevance and availability. They are presented in Table 6-1. The description of the test setups can be found in [45] and [38].

Table 6-1 Overview of the selected model tests

Test	Configuration	Flow conditions
NDP 38m [45]	Bare	Uniform/Sheared
	Partial strake coverage	Uniform/Sheared
NDP 38m staggered buoyancy elements [38]	Staggered buoyancy elements	Uniform

6.1 Validation against NDP 38m high mode VIV tests

The TD empirical parameters derived in the Section 5.1.2 and 5.2.1 have been applied to predict VIV response of an elastic pipe divided into two segments, 59% of the length without strakes and 41% of the length covered by strakes.

The dominating frequency and the maximum fatigue damage for each test case have been extracted based on the definition in Section 3.2. They are compared with TD prediction results in Figure 6-1 to Figure 6-8.

As shown, the dominating response frequency is accurately predicted. The predicted maximum fatigue damage is in general within a factor of five compared to the measured values, as indicated by the yellow and blue lines in the figures. The predicted displacement and mode are also in good agreement with the measurements.

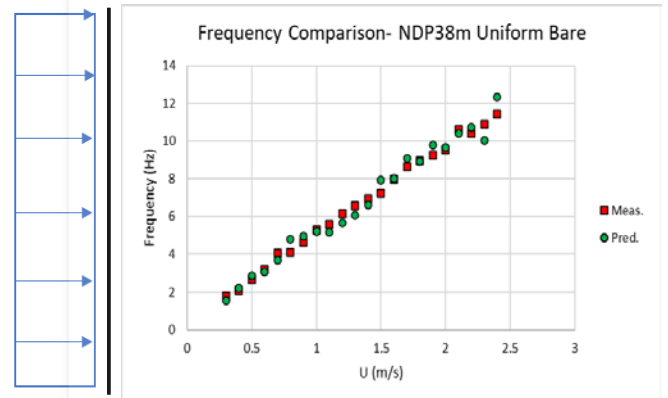### 1) Dominating frequency comparison

Figure 6-1 Comparison of dominating frequency prediction against model test data for a bare pipe in uniform flow
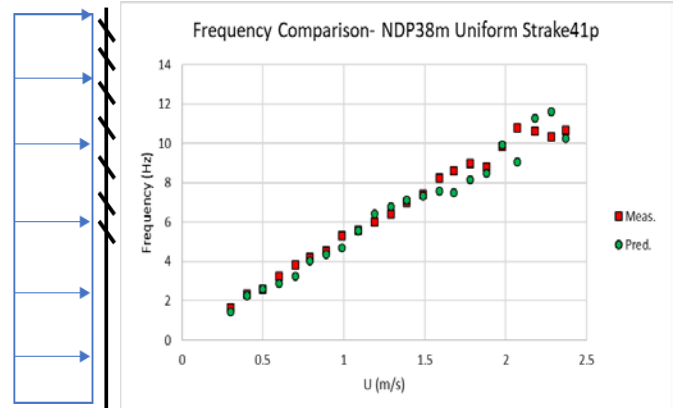

Figure 6-2 Comparison of dominating frequency prediction against model test data for a pipe with 41% strake coverage in uniform flow
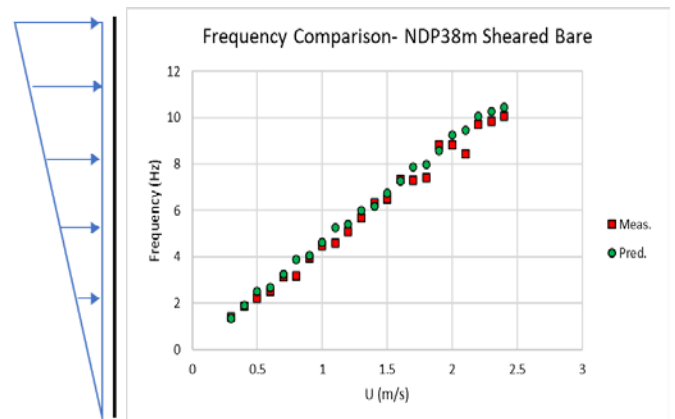

Figure 6-3 Comparison of dominating frequency prediction against model test data for a bare pipe in sheared flow
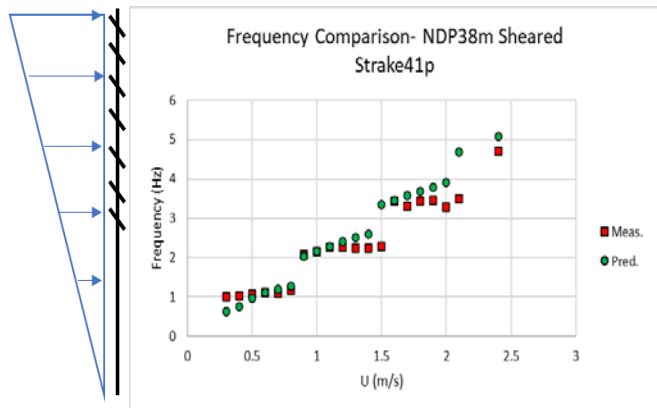
Figure 6-4 Comparison of dominating frequency prediction against model test data for a pipe with 41% strake coverage in sheared flow
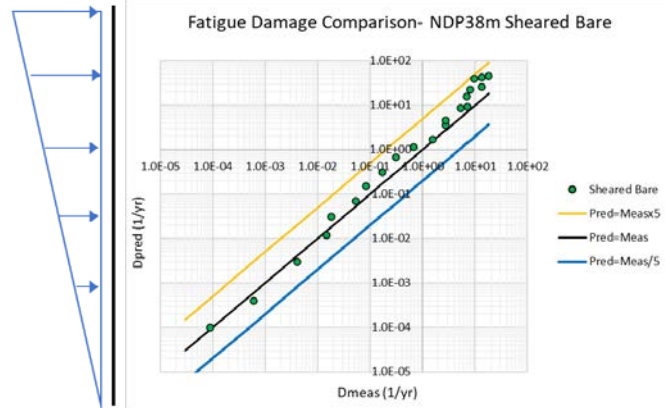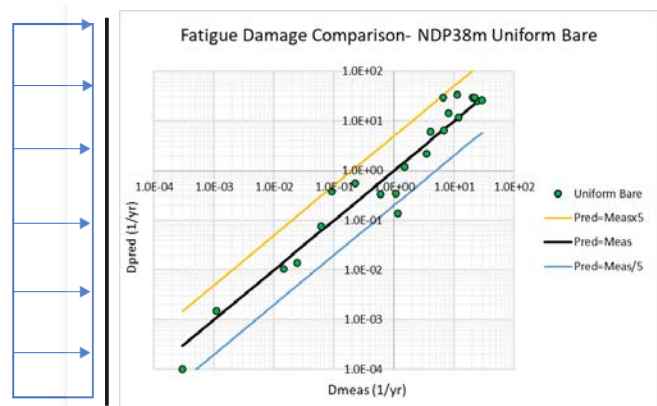
2) **Maximum fatigue damage comparison**

Figure 6-5 Comparison of maximum fatigue damage prediction against model test data for a bare pipe in uniform flow
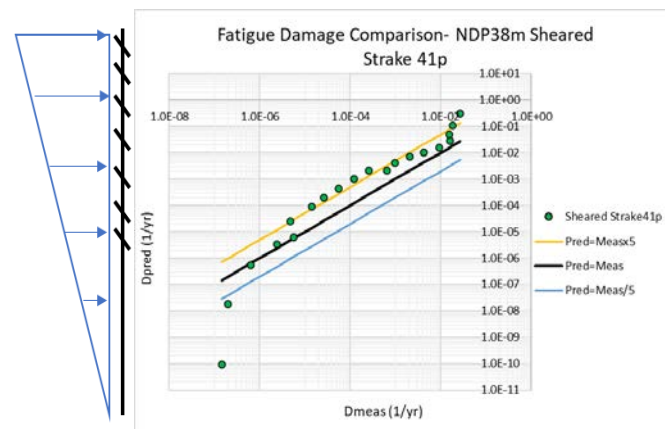

Figure 6-6 Comparison of maximum fatigue damage prediction against model test data for a pipe with 41p strake in uniform flow

Figure 6-7 Comparison of maximum fatigue damage prediction against model test data for a bare pipe in sheared flow

Figure 6-8 Comparison of maximum fatigue damage prediction against model test data for a pipe with 41% strake coverage in sheared flow
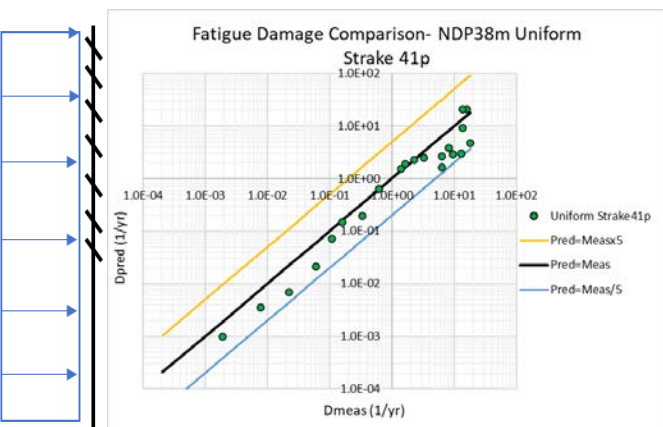
6.2 Validation against NDP 38m staggered buoyancy VIV tests

The TD empirical parameters derived in the Section 5.2 have been applied to predict VIV response of an elastic pipe with staggered buoyancy elements.

The measured dominating frequency and the maximum fatigue damage for each test case are compared with TD prediction results in Figure 6-9 to Figure 6-12.
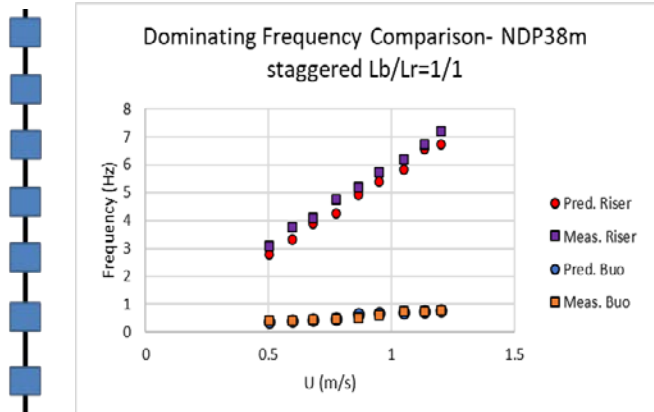
Figure 6-9 Comparison of dominating frequency prediction against model test data for a riser with staggered buoyancy elements ($L_b/L_r = 1/1$) in uniform flow

Figure 6-10 Comparison of maximum fatigue damage prediction against model test data for a riser with staggered buoyancy elements ($L_b/L_r = 1/1$) in uniform flow
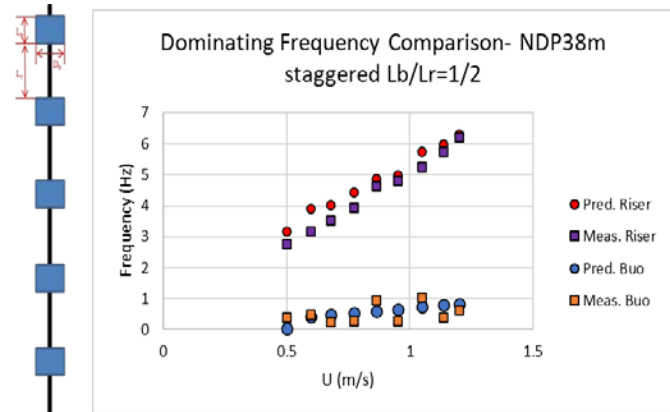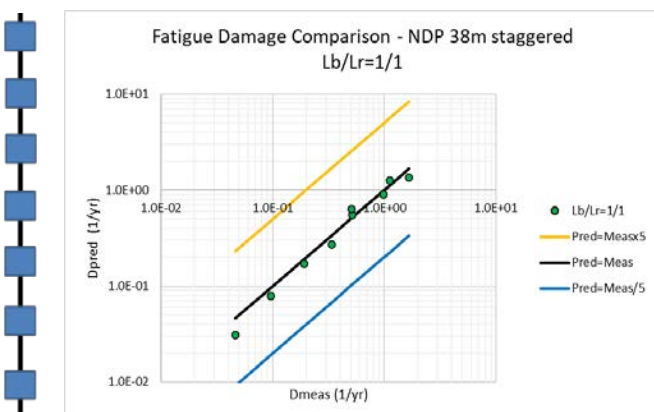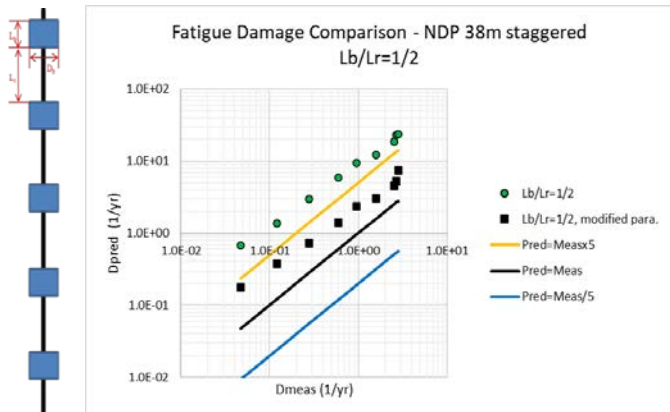

Figure 6-11 Comparison of dominating frequency prediction against model test data for a riser with staggered buoyancy elements ($L_b/L_r = 1/2$) in uniform flow

Figure 6-12 Improved prediction of maximum fatigue damage for a riser with staggered buoyancy elements ($L_b/L_r = 1/2$) in uniform flow

As shown in Figure 6-9, the dominating response frequency of the bare riser section and the buoyancy element is accurately predicted for the configuration $L_b/L_r = 1/1$. The predicted maximum fatigue damage is in good agreement with the measurement, as shown in Figure 6-10.

The frequency prediction for the configuration $L_b/L_r = 1/2$ (Figure 6-11) shows good agreement with the measured values. The fatigue damage is over-predicted by a factor of 7 – 15.

However, the test with the flexible pipe shows that there are increasingly more IL responses as the spacing between the buoyancy elements increases [38]. This means that the hydrodynamic parameters obtained from pure CF motion test can contribute to the uncertainty in the prediction.

A modified set of the hydrodynamic parameters of the bare section has been applied with reduced excitation on the bare riser section and the fatigue damage prediction is shown to be improved.

7   SUMMARY

In the present study, the empirical time domain VIV prediction tool VIVANA-TD has been evaluated:
1) Empirical parameters have been derived based on extensive evaluation of rigid cylinder and elastic pipe tests.
2) Validation has been carried out for constant flow conditions for:
   - Bare pipe, pipe with partial strake coverage and riser model with staggered buoyancy elements
   - Uniform/sheared flow conditions

It was found that:
- The dominating frequency is accurately predicted
- The predicted displacement and mode are also in good agreement with the measurements.
- The predicted maximum fatigue damage is in general within a factor of 5 compared to the measurements, except for the staggered buoyancy elements configuration with $L_b/L_r = 1/2$.

This shows that the present TD model can represent reasonably the VIV loads and that the prediction has good agreement with measurements in general.

Further work includes:

1) Validation of VIVANA-TD for oscillatory flow conditions
2) Consolidation of the empirical basis and modelling methods
3) Development of guidance on the time domain VIV calculation for deep-water SLWRs
4) Development of a road map towards future integrated model for combined waves and VIV loads

8 ACKNOWLEDGEMENTS

9 REFERENCES

[1] Thorsen, M.J. Time Domain Analysis of Vortex-Induced Vibrations. PhD thesis, 2016.

[2] Yin, D., Lie, H., Wu, J. 2019. Structural and Hydrodynamic Aspects of Steel Lazy Wave Riser in Deepwater. ASME. J. Offshore Mech. Arct. Eng. April 2020; 142(2): 020801. https://doi.org/10.1115/1.4045333.

[3] Ulveseter, J.V. Advances in semi-empirical time domain modelling of vortex-induced vibrations. PhD thesis, 2018.

[4] Thorsen, M.J., S. Sævik, and C.M. Larsen, Time domain simulation of vortex-induced vibrations in stationary and oscillating flows. Journal of Fluids and Structures, 2016. 61: p. 1-19.

[5] Ulveseter, J.V., Thorsen, M.J., S. Sævik, and C.M. Larsen, Time domain simulation of riser VIV in current and irregular waves. Marine Structures, 2018. 60: p. 241-260.

[6] Thorsen, M.J., S. Sævik, and C.M. Larsen, Fatigue damage from time domain simulation of combined in-line and cross-flow vortex-induced vibrations. Marine Structures, 2015. 41: p. 200-222.

[7] Ulveseter, J.V., Thorsen, M.J., S. Sævik, and C.M. Larsen, Stochastic modelling of cross-flow vortex-induced vibrations. Marine Structures, 2017. 56: p. 260-280.

[8] Bourget, R., Karniadakis, G.E., Triantafyllou, M.S., 2013. Multi-frequency vortex-induced vibrations of a long tensioned beam in linear and exponential shear flows. Journal of Fluid and Structures, Issue 41, pp. 33-42.

[9] Bourget, R., Karniadakis, G. E. & Triantafyllou, 2011. Vortex-induced vibrations of long flexible cylinder in sheared flow. Journal of fluid mechanics, Volum 677, pp. 342-382.

[10] Drengsrud, H., Systematic Evaluation of VIV Prediction for Riser with Partial Strake Coverage, Master Thesis, NTNU, Trondheim 2019.

[11] Nestegård, A., Voie, P.E. and Sødahl, N. Hydrodynamic coefficients for straked risers. ASME 2014, 33rd International Conference on Ocean, Offshore and Arctic Engineering, 6A: Pipeline and Riser Technology, 2014.

[12] SINTEF Ocean. RIFLEX v4.14, Theory Manual. 2019.

[13] SINTEF Ocean. SIMA v3.7.2, 2019.

[14] SINTEF Ocean. VIVANA v4.14, 2019

[15] SINTEF Ocean. VIVANA-TD, Theory Manual. 2020.

[16] Zheng H, Price R, Modarres-Sadeghi, Y., Triantafyllou, G.S., and Triantafyllou, M.S. Vortex-Induced Vibration Analysis (VIVA) Based on Hydrodynamic Databases. ASME 2011 30th International Conference on Ocean, Offshore and Arctic Engineering, 2011, Vol. 7: CFD and VIV, pp. 657–663. doi:10.1115/OMAE2011-50192.

[17] Gopalkrishnan, R. Vortex-Induced Forces on Oscillating Bluff Cylinders. PhD thesis, Massachusetts Institute of Technology, Cambridge, MA, USA, 1993.

[18] Wu, J.; Larsen, C.M.; Lie, H. Estimation of hydrodynamic coefficients for VIV of slender beam at high mode orders. ASME 2010 29th International Conference on Ocean, Offshore and Arctic Engineering, 2010.

[19] Campbell, M., Tognarelli, M. Drilling Riser VIV: Fact or Fiction? IADC/SPE Drilling Conference and Exhibition, 2010.

[20] Wu, J., Yin, D., Lie, H., Larsen, C.M., Baarholm, R.J., Liapis, S. On the Significance of the Higher-Order Stress in Riser Vortex-Induced Vibrations Responses. Journal of Offshore Mechanics and Arctic Engineering 2018, 456141, 011705. doi:10.1115/1.4040798.

[21] Lie, H., Braaten, H., Jhingran, V., Sequeiros, O.E., Vandiver, J.K. Comprehensive Riser VIV Model Tests in Uniform and Sheared Flow. Proceedings of the 31st International Conference on Ocean, Offshore and Arctic Engineering, 2012.

[22] Tognarelli, M., Slocum, S., Frank, W., Campbell, R.B. VIV Response of a Long Flexible Cylinder in Uniform and Linearly Sheared Currents. Offshore Technology Conference, 2004.

[23] Larsen, C.M., Zhao, Z., Lie, H. Frequency Components of Vortex Induced Vibartions in Sheared Current. Proceedings of the ASME 2012 31st International Conference of Ocean, Offshore and Arctic Engineering, 2012.

[24] Swithenbank, S.B. Dynamics of Long Flexible Cylinders at High-Mode Number in Uniform and Sheared Flows. PhD thesis, Massachusetts Institute of Technology, 2007.

[25] Voie, P.E., Larsen, C.M., Wu, J., Resvanis, T. Guideline on analysis of vortex-induced vibrations. Technical Report 2016-0226, Rev. 0, Statoil Petroleum AS, 2016.

[26] Wu, J., Lie, H., Larsen, C.M., Liapis, S., Baarholm, R. Vortex-induced vibration of a flexible cylinder: Interaction of the in-line and cross-flow responses. Journal of Fluids and Structures 2016, 63, 238 – 258. doi:http://dx.doi.org/10.1016/j.jfluidstructs.2016.03.001.

[27] Mukundan, H., Chasparis, F., Hover, F.S., Triantafyllou, M.S. Optimal lift force coefficient databases from riser experiments. Journal of Fluids and Structures 2010, 160–175. doi:10.1016/j.jfluidstructs.2009.09.004.

[28] Voie, P., Wu, J., Resvanis, T., Larsen, C., Vandiver, K., Triantafyllou, M. Consolidation of empirics for calculation of VIV response. ASME 2017 36th International Conference

on Ocean, Offshore and Arctic Engineering, 2017, Number OMAE2017-61362 in Prof. Carl Martin Larsen and Dr. Owen Oakley Honoring Symposia on CFD and VIV.

[29] Yin, D. Experimental and Numerical Analysis of Combined In-line and Cross-flow Vortex-Induced Vibrations. PhD thesis, Norwegian University of Science and Technology, Trondheim, Norway, 2013.9.

[30] Dahl, J.M. Vortex-Induced Vibration of a Circular Cylinder with Combined In-line and Cross-flow Motion. PhD thesis, Center for Ocean Engineering, Department of Mechanical Engineering, MIT, Webb Institute, Glen Cove, NY, USA, 2008

[31] Lie, H., Mo, K., Vandiver, K., "VIV Model Test of Bare- and Staggered Buoyancy Riser in a Rotating Rig", OTC, Houston, 1998

[32] Jhingran, V., Zhang, H.P., Lie, H., Braaten, H., and Vandiver, J.K., "Buoyancy Spacing Implications for Fatigue Damage due to Vortex-Induced Vibrations on a Steel Lazy Wave Riser (SLWR)". Offshore Technology Conference, OTC23672, May 2012, Houston, USA.

[33] Rao, Z., Vandiver, J.K., Jhingran, V., Vortex induced vibration excitation competition between bare and buoyant segments of flexible cylinders, Ocean Engineering, Volume 94, 15 January 2015, Pages 186-198.

[34] Vikestad, K. Multi-frequency response of a cylinder subjected to vortex shedding and support motions. PhD thesis, Norwegian University of Science and Technology, 1998.

[35] Oyvind, S. & Franz, H. & Triantafyllou, M.S. (2003). Force-Feedback Control in VIV Experiments. 685-695. 10.1115/OMAE2003-37340.

[36] Khalak, A. and Williamson, K. Dynamics of a hydroelastic cylinder with very low mass and damping. Journal of Fluids and Structures, 10:455{472, 1996.

[37] Sarpkaya, T. Hydrodynamic damping, flow-induced oscillations, and bi-harmonic response. ASME Journal of Offshore Mechanics and Arctic Engineering, 117:232-238, 1995.

[38] Wu, J., Lie, H., Constantinides, Y., & Baarholm, R. (2016). NDP riser VIV model test with staggered buoyancy elements. Bushan, the South Korea: 35th International Conference on Ocean, Offshore and Arctic Engineering, OMAE2016-54503.

[39] Wu, J., Lie, H., Fu, S., Constantinides, Y., Baarholm, R. (2017) VIV Responses of Riser with Buoyancy Elements: Forced Motion Test and Numerical Prediction. Trondheim, Norway: 36th International Conference on Ocean, Offshore and Arctic Engineering, OMAE2017-61768.

[40] Wu, J., Lekkala, M.R., Ong, M.C., Passano, E., Voie, P. Prediction of Combined Inline and Crossflow Vortex-Induced Vibrations Response of Deepwater Risers. J. Offshore Mech. Arct. Eng. Aug 2019, 141(4): 041803.

[41] Søreide, M. (2003) Experimental Investigation of In-line and Cross-flow VIV. Proceedings of the Thirteenth International Offshore and Polar Engineering Conference.

[42] Vandiver, J., & Resvanis, T. (2015). Improving the state of the art of high Reynolds number VIV model testing of ocean risers. Cambridge, MA, USA: Massachusets Institute of Technology.

[43] Yin, D., Lie, H., Baarholm, R. (2017). Prototype Reynolds Number VIV Tests on a Full-scale Rigid Riser. Journal of Offshore Mechanics and Arctic Engineering. 140. 10.1115/1.4037538.

[44] Ding, Z., Balasubramanian, S., Lokken, R. & Yung, T.-W., 2004. Lift and damping characteristics of bare and straked cylinder at riser scale. Houston, OTC.

[45] Trim AD, Braaten H, Lie H, Tognarelli MA. Experimental investigation of vortex-induced vibration of long marine risers. Journal of Fluid Structures 2005,21:335-61.

[46] Vandiver JK, Marcollo H, Swithenbank S, Jhingran V. High mode number vortex-induced vibration field experiments. In: Proc. 2005 Offshore Tech Conf, Houston, USA, 2005. OTC Paper No. 17383.

[47] Senga, H., Larsen, C.M. Forced motion experiments using cylinders with helical strakes. Journal of Fluids and Structures, 68:279-294, 2017.

[48] Constantinides, Y., Cao, P., Cheng, J., Fu, S., and Kusinski, G. Steel Lazy Wave Riser Tests in Harsh Offshore Environment, in ASME 2016 35th International Conference on Ocean, Offshore and Arctic Engineering. 2016: Busan, South Korea.

[49] Wu, J., Maincon, P., Larsen, C.M., and Lie, H. "VIV Force Identification Using Classical Optimal Control Algorithm." Proceedings of the ASME 2009 28th International Conference on Ocean, Offshore and Arctic Engineering. Volume 5: Polar and Arctic Sciences and Technology, CFD and VIV. Honolulu, Hawaii, USA. May 31–June 5, 2009. pp. 559-570. ASME. https://doi.org/10.1115/OMAE2009-79568.